Illumination of the Endogenous Insulin-Regulated TBC1D4 Interactome in Human Skeletal Muscle

Jeppe K. Larsen,[1,2] Magnus R. Larsen,[1] Jesper B. Birk,[1] Dorte E. Steenberg,[1] Janne R. Hingst,[1] Kurt Højlund,[3,4] Alexandra Chadt,[5,6] Hadi Al-Hasani,[5,6] Atul S. Deshmukh,[2] Jørgen F.P. Wojtaszewski,[1] and Rasmus Kjøbsted[1]

Diabetes 2022;71:906–920 | https://doi.org/10.2337/db21-0855

Insulin-stimulated muscle glucose uptake is a key process in glycemic control. This process depends on the redistribution of glucose transporters to the surface membrane, a process that involves regulatory proteins such as TBC1D1 and TBC1D4. Accordingly, a TBC1D4 loss-of-function mutation in human skeletal muscle is associated with an increased risk of type 2 diabetes, and observations from carriers of a TBC1D1 variant associate this protein to a severe obesity phenotype. Here, we identified interactors of the endogenous TBC1D4 protein in human skeletal muscle by an unbiased proteomics approach. We detected 76 proteins as candidate TBC1D4 interactors. The binding of 12 of these interactors was regulated by insulin, including proteins known to be involved in glucose metabolism (e.g., 14-3-3 proteins and α-actinin-4 [ACTN4]). TBC1D1 also coprecipitated with TBC1D4 and vice versa in both human and mouse skeletal muscle. This interaction was not regulated by insulin or exercise in young, healthy, lean individuals. Similarly, the exercise- and insulin-regulated phosphorylation of the TBC1D1-TBC1D4 complex was intact. In contrast, we observed an altered interaction as well as compromised insulin-stimulated phosphoregulation of the TBC1D1-TBC1D4 complex in muscle of obese individuals with type 2 diabetes. Altogether, we provide a repository of TBC1D4 interactors in human and mouse skeletal muscle that serve as potential regulators of TBC1D4 function and, thus, insulin-stimulated glucose uptake in human skeletal muscle.

Reduced insulin-stimulated skeletal muscle glucose uptake is a hallmark of various metabolic disorders, including type 2 diabetes (1). The increase in muscle glucose permeability evoked by insulin stimulation is partly mediated through an IRS1-, PI3K-, and Akt-dependent signaling pathway (2). Akt has been shown to inhibit the activity of the RabGTPase-activating protein (RabGAP) TBC1D4 (also known as AS160) by multisite phosphorylation affecting in vivo insulin-stimulated GLUT4 translocation and glucose uptake in mature skeletal muscle (3,4). In humans, a common Greenlandic and Canadian Inuit loss-of-function mutation in *TBC1D4* is associated with poor postprandial glucose handling and a 10-times increased risk of type 2 diabetes (5,6). Interestingly, the closely related RabGAP TBC1D1 also displays regulatory actions in contraction and insulin-stimulated glucose uptake (7,8). Two studies have found that the TBC1D1 R125W variant is associated with severe obesity in human cohorts (9,10). Altogether, these observations underline the clinical importance of studying TBC1D1 and TBC1D4 in human skeletal muscle.

Skeletal muscle TBC1D4 has been proposed to function as a convergence point for insulin- and exercise-induced

[1]August Krogh Section for Molecular Physiology, Department of Nutrition, Exercise and Sports, Faculty of Science, University of Copenhagen, Copenhagen, Denmark
[2]Novo Nordisk Foundation Center for Basic Metabolic Research, University of Copenhagen, Copenhagen, Denmark
[3]Steno Diabetes Center Odense, Odense University Hospital, Odense, Denmark
[4]Department of Clinical Research, University of Southern Denmark, Odense, Denmark
[5]German Diabetes Center, Leibniz Center for Diabetes Research at the Heinrich Heine University Düsseldorf, Düsseldorf, Germany
[6]German Center for Diabetes Research (DZD), München-Neuherberg, Germany

Corresponding authors: Rasmus Kjøbsted, rasmus.kjobsted@nexs.ku.dk, and Jørgen F.P. Wojtaszewski, jw@nexs.ku.dk

Received 22 September 2021 and accepted 15 February 2022

This article contains supplementary material online at https://doi.org/10.2337/figshare.19184333.

signaling (11). We recently showed that genetic ablation of TBC1D4 in mouse skeletal muscle abolishes the insulin-sensitizing effect of contraction as well as of the AMP-activated protein kinase (AMPK) activator AICAR (12). Considering the evidence suggesting a role of TBC1D4 phosphorylation for insulin and exercise-stimulated glucose uptake, studies on protein interactors of TBC1D4 implicated in these processes are lacking. The most well-known TBC1D4 binding partners are the 14-3-3 scaffold proteins, which are recruited upon insulin stimulation when TBC1D4 is phosphorylated (13). Cell studies report that binding of 14-3-3 proteins inhibits the RabGTPase stimulatory actions of TBC1D4, thereby releasing the brake on Rab proteins (14,15). In line, disruption of the 14-3-3 binding to TBC1D4 reduces insulin-stimulated GLUT4 translocation and glucose uptake in mature skeletal muscle (4).

Proteomics that investigates protein-protein interactions have readily been applied to cell systems with the use of exogenous epitope tags in combination with protein overexpression (16,17). However, the exogenous tags and elevated expression levels might represent nonphysiological conditions that result in an altered interaction profile. Here we explored endogenous TBC1D4 interacting partners in human skeletal muscle by antibody-based immunoprecipitation (IP) coupled to mass spectrometry (MS) and sought to identify interaction partners regulated during physiological hyperinsulinemic clamp conditions in healthy, lean subjects. We identified known and novel interaction partners of TBC1D4 with a role in glucose metabolism of which a subset was regulated by insulin. As TBC1D1 was found to be highly associated with TBC1D4, we furthermore investigated this interaction during insulin-stimulated conditions and after exercise in both healthy individuals and patients with type 2 diabetes.

RESEARCH DESIGN AND METHODS

The experimental workflow is presented in Fig. 1*A*. Human skeletal muscle biopsy specimens from vastus lateralis were obtained from previous studies, as described below. In parallel, skeletal muscle from wild-type (WT) and *Tbc1d4* whole-body knock-out (KO) animals in the basal nonstimulated state was harvested (12). Skeletal muscle samples were homogenized, and TBC1D4 was immunoprecipitated, followed by extensive washing. Proteins were on-bead digested with trypsin, and peptides were analyzed by an MS-based setup in a data-dependent acquisition mode. Bioinformatics were performed using MaxQuant and Perseus software to identify TBC1D4 interactors (18,19). Candidate interactors were validated by Western blotting and investigated under various physiological settings, including before and after hyperinsulinemic-euglycemic clamp conditions as well as before and after a single bout of exercise.

Subjects

For human data shown in Fig. 1, muscle biopsy specimens from six young (25 ± 1 years), lean (23.4 ± 0.4 kg · m^{-2}), and healthy male subjects were used. The study was approved by the Regional Ethics Committee for Copenhagen (H-6-2014-038) and described in detail in Steenberg et al. (20). In short, muscle biopsy specimens were obtained from vastus lateralis in the rested nonstimulated state and at the end of a 2-h hyperinsulinemic-euglycemic clamp (plasma insulin ∼117 μIU · mL^{-1} over the last 40 min of the clamp).

For human data shown in Figs. 2*A–D*, 3*A* and *B*, and 4*A–C*, muscle biopsy specimens from two independent cohorts were used: in total 11 young (26 ± 1 years), lean (23.3 ± 0.5 kg · m^{-2}), and healthy male subjects. The studies were approved by the Regional Ethics Committee for Copenhagen (H-6-2014-038 and H-4-2013-071) and described in detail in Steenberg et al. (21) and Hingst et al. (22). In short, muscle biopsy specimens were obtained from vastus lateralis before and at the end of a 2-h hyperinsulinemic-euglycemic clamp (plasma insulin: cohort 1 [21], ∼129 μIU · mL^{-1} and cohort 2 [22], ∼100 μIU · mL^{-1} over the last 40 min of the clamp).

For human data shown in Figs. 3*C–E* and 4*D–F* muscle biopsy specimens were obtained from eight young (23.6 ± 0.9 years), lean (23.3 ± 0.6 kg · m^{-2}), and healthy male subjects. The studies were approved by the Regional Ethics Committee for Copenhagen (H-2-20120085) and described in detail in Kristensen et al. (23). In short, muscle biopsy specimens were obtained from vastus lateralis before and at the end of a single exercise bout. The exercise protocol consisted of 30 min of interval cycling exercise consisting of six high intensity bouts of 1.5 min (workload ∼100% VO_2peak) intervened with 2.5 min of active recovery (workload 40% VO_2peak).

For human data shown in Supplementary Fig. 2*A–C*, muscle biopsy specimens were obtained from the same healthy male subjects as described above. The studies were approved by the Regional Ethics Committee for Copenhagen (H-2-2012-085) and described in details in Kristensen et al. (23). In short, muscle biopsy specimens were obtained from vastus lateralis before and at the end of a single exercise bout. The exercise protocol consisted of 30 min of continuous cycling exercise at ∼70% of VO_2peak.

For human data shown in Fig. 5 muscle biopsy specimens from seven young (25 ± 1 years), lean (23.4 ± 0.4 kg · m^{-2}), and healthy male subjects were used. The study was approved by the Regional Ethics Committee for Copenhagen (H-6-2014-038) and described in detail in Steenberg et al. (20). In short, subjects arrived at the laboratory 1 h after eating a small breakfast meal (5% of daily energy intake) and exercised one leg for 1 h (80% of peak work load interspersed with 3 × 5 min at 100% of peak work load), followed by 4 h of rest. After the resting period, muscle biopsy specimens were obtained from vastus lateralis of both legs (rested and prior exercised leg). Then the subjects underwent a 2-h hyperinsulinemic-euglycemic clamp (plasma insulin ∼117 μIU · mL^{-1} over the last 40 min

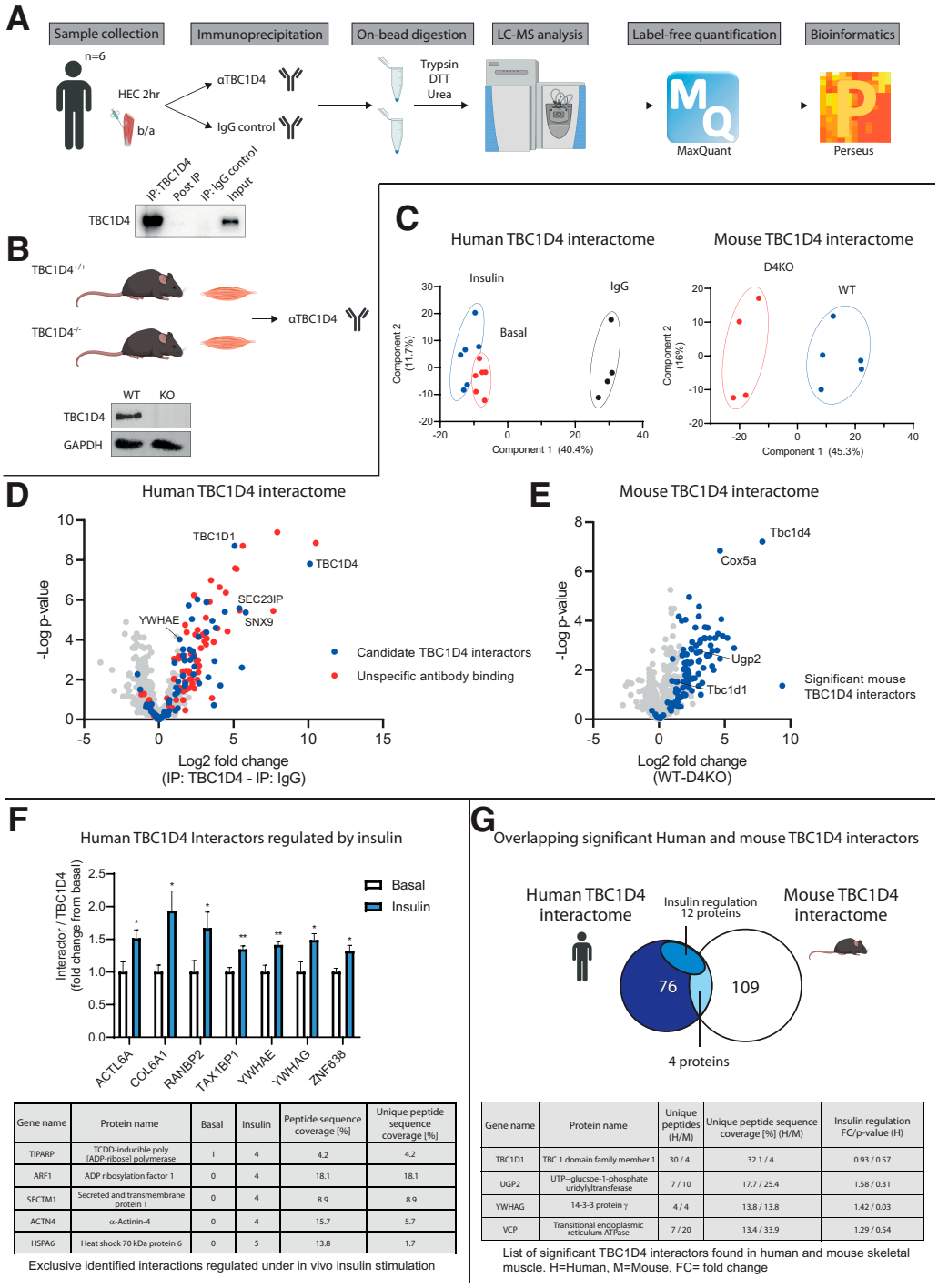

Gene name	Protein name	Basal	Insulin	Peptide sequence coverage [%]	Unique peptide sequence coverage [%]
TIPARP	TCDD-inducible poly [ADP-ribose] polymerase	1	4	4.2	4.2
ARF1	ADP ribosylation factor 1	0	4	18.1	18.1
SECTM1	Secreted and transmembrane protein 1	0	4	8.9	8.9
ACTN4	α-Actinin-4	0	4	15.7	5.7
HSPA6	Heat shock 70 kDa protein 6	0	5	13.8	1.7

Exclusive identified interactions regulated under in vivo insulin stimulation

Gene name	Protein name	Unique peptides (H/M)	Unique peptide sequence coverage [%] (H/M)	Insulin regulation FC/p-value (H)
TBC1D1	TBC 1 domain family member 1	30 / 4	32.1 / 4	0.93 / 0.57
UGP2	UTP–glucose-1-phosphate uridylyltransferase	7 / 10	17.7 / 25.4	1.58 / 0.31
YWHAG	14-3-3 protein γ	4 / 4	13.8 / 13.8	1.42 / 0.03
VCP	Transitional endoplasmic reticulum ATPase	7 / 20	13.4 / 33.9	1.29 / 0.54

List of significant TBC1D4 interactors found in human and mouse skeletal muscle. H=Human, M=Mouse, FC= fold change

Figure 1—Identification of TBC1D4 interacting partners in human skeletal muscle. Experimental approach for mapping the TBC1D4 interactome in human skeletal muscle before and after (b/a) a hyperinsulinemic-euglycemic clamp (HEC) (*A*) and in WT and TBC1D4 whole-body KO mouse skeletal muscle at basal (*B*). DTT, dithiothreitol. *C*: Principal component analysis plot including principal components 1 and 2 on all quantified proteins in human (left) and mouse (right) muscle. Dots represent individual samples, and colored circles are manually inserted. Volcano plots based on the Student *t* test for the human (*D*) and mouse TBC1D4 interactome (*E*) with $\log_2$-fold change difference (human: TBC1D4 IP – IgG IP or mouse: WT-TBC1D4 KO) on the *x*-axis and $-\log_{10} P$ values on the *y*-axis. Significant interactors are marked in blue. Owing to low abundance and exclusive quantification of some interactors, imputation of missing values in the corresponding control samples can make a significant interactor appear with a negative $\log_2$ difference. *F*: Proteins in which their interaction with TBC1D4 is regulated by insulin stimulation either by Student *t* test (bar graph with mean ± SEM) or exclusive identification (Table). *G*: Venn diagram illustrating significant TBC1D4 interactors found in human, mouse, or both species. Detailed information on identification of interactors found in both human and mouse muscle.

of the clamp), and additional biopsy specimens were obtained from both legs by the end of the clamp.

For human data shown in Fig. 6, muscle biopsy specimens were obtained from 10 (4 female, 6 male) middle-aged (50 ± 1 years), obese (33 ± 1 kg · m^{-2}) individuals with type 2 diabetes (HbA_{1c} 7.8% ± 0.5%) and 10 (5 female, 5 male) aged-matched (51 ± 1 years) healthy, lean (24 ± 1 kg · m^{-2}) control subjects. The study was approved by the Regional Ethics Committee and described in details in Højlund et al. (24). In short, muscle biopsy specimens were obtained from vastus lateralis before and at the end of a 4-h hyperinsulinemic-euglycemic clamp (serum insulin concentration at steady state, ∼54 μU/mL).

Biopsy Specimens

Muscle biopsy specimens were obtained from vastus lateralis using the Bergstrom needle technique with suction (25).

Animals

All animal experiments were approved by the Danish Animal Experiments Inspectorate (License no. 2014-15-2934-01037). Whole-body TBC1D4-KO and whole-body TBC1D1-KO female mice, including wild-type (WT) littermates, on a C57BL/6J background (26) had free access to standard rodent chow and water and were group housed at a 12:12-h light-dark cycle. Fed mice with an age of 16 ± 2 weeks were anesthetized by an intraperitoneal injection of pentobarbital (10 mg/100 g body wt). Tibialis anterior muscle was dissected and immediately frozen in liquid nitrogen for later analyses.

Muscle Processing and IP

Both human and mouse muscles were homogenized in lysis buffer and prepared as muscle lysates as previously described (27). The bicinchoninic acid method was used to determine total protein abundance in muscle lysates. TBC1D4 was immunoprecipitated with a C-terminal anti-TBC1D4 antibody (ab24469, Abcam) by protein G covalent conjugated agarose beads (Millipore, no. 16-266) from 400 μg of muscle lysate and incubated overnight at 4°C. The following day, agarose beads were centrifuged, and supernatant was collected. Beads were washed twice in lysis buffer, twice in NP-40 buffer (150 mmol/L NaCl, glycerol 5%, 0.05% NP40, and 50 mmol/L Tris-HCl; pH 7.5) and four times in a NaCl buffer (150 mmol/L NaCl, glycerol 5%, and 50 mmol/L Tris-HCl; pH 7.5).

SDS-PAGE and Western Blot Analyses

Lysates were boiled in Laemmli buffer and subjected to SDS-PAGE and immunoblotting, as previously described (27). In brief, SDS-PAGE separated proteins were transferred to a polyvinylidene fluoride membrane, blocked for 10 min in Tris-buffered saline with TWEEN (TBS-T) containing 3% BSA or 2% skim milk and incubated overnight with primary antibody at 4°C. Membranes were then washed in TBS-T three times for 5 min and subjected to secondary antibody (1:5000) for 45 min at room temperature. Lastly, membranes were washed in TBS-T three times for 10 min before being incubated with enhanced chemiluminescence (Luminata Forte Western horseradish peroxidase substrate, Bio-Rad). Images were acquired on a Bio-Rad Chemi Doc XRS+ system. In order to relate phosphorylated protein to total protein abundance, membranes were stripped in a Tris buffer (pH 6.7) consisting of 2% SDS, 62.5 mmol/L Tris HCl, and freshly added 2-mercaptoethanol for 1 h at 50°C, followed by 1 h at room temperature on a rocking platform. Membranes were always checked with secondary antibody for complete stripping of the primary antibody.

Antibodies

Primary antibodies against pTBC1D4-Ser318 (8619), pTBC1D4-Thr642 (8881), pTBC1D1-Thr596 (6927S), pAkt-Thr308 (9275), pAkt-Ser473 (4271L), Akt2 (3063), pAMPK-Thr172 (2531), and GAPDH (2118) were from Cell Signaling Technology. Antibodies against pTBC1D1-Ser237 (07-2268) and AMPKa2 (SC-19131) were from Millipore and Santa Cruz Biotechnology, respectively. Antibody against TBC1D1 for IP and immunoblot (22124-1-AP) was from ProteinTech. pTBC1D4-Ser704 was detected using antibody donated by Dr. Laurie J. Goodyear (28). Antibody for IP of TBC1D4 (C-terminal: ab24469) and immunoblot (N-terminal: ab189890) were from Abcam.

Proteomics Sample Preparation and Liquid Chromatography–MS Analysis

After the last IP wash, proteins were on-bead digested by trypsin, as previously described (29). Peptides were desalted on 2xC18 StageTips. Tryptic peptides were separated on an in-house packed 15-cm column (inner diameter, 75 μm, 1.8 μm C18 beads; Dr. Maisch GmbH) using the Easy nano-flow high-performance liquid chromatography system. Peptides were loaded on the column in buffer A (0.5% formic acid) and eluted with a 100-min linear gradient from 2 to 40% buffer B (80% acetonitrile, 0.5% formic acid). The high-performance liquid chromatography system was coupled via a nano electrospray ion source to a Q Exactive HFX Hybrid Quadrupole-Orbitrap Mass Spectrometer (Thermo Fisher Scientific, Bremen, Germany). Mass spectra were generated by the data-dependent acquisition with automatic switching between MS and tandem MS (MS/MS). Precursor ions were picked using the top-15 method. Tandem spectra were generated using high collision dissociation (27 normalized collision energy). MS and MS/MS spectra were acquired at 60,000 and 15,000 resolutions respectively using the Orbitrap analyzer.

Data Analysis

Raw mass spectra were quantified in MaxQuant 1.6.01 software with default parameters (18). These include minimal peptide length of seven amino acids, a maximum of two miscleavages allowed, and a false-discovery rate (FDR) of 1% for peptide and protein identification. The match-between-

runs function was enabled, and the retention time window was set to 30 s. Label-free quantification (LFQ) was performed using the built-in MaxLFQ algorithm in MaxQuant.

Bioinformatics Analysis and Statistics

MaxQuant-derived LFQ intensities were imported to Perseus 1.6.1.1 software (19). Contaminants and reverse sequence identification were excluded from further data analysis. For the human TBC1D4 interactome, 16 samples were measured (6 basal TBC1D4 IPs, 6 insulin TBC1D4 IPs, and 4 IgG control IPs). For the mouse TBC1D4 interactome, 10 samples were measured (5 TBC1D4 IPs in both WT and TBC1D4 KO muscle lysate). One TBC1D4-KO sample was excluded in the analysis due to technical reasons. Only proteins quantified in three or more biological replicates in at least one group (specific IP group or control group) were used for further analysis. To restore the lower tail of the Gaussian distribution, missing values (not a number [NaN]) were imputed with random generated numbers separately from each sample with a 1.8 SD downshift of the mean and a SD of 30%. Principal component analysis was performed in Perseus software.

To be considered a candidate TBC1D4 interactor, proteins must be *1*) exclusively detected in TBC1D4 IP reactions in three of six human samples or three of five WT mouse samples or *2*) enriched in TBC1D4 IP samples compared with IgG control IP samples by at least a 1.5-fold change and significant on a 5% FDR (permutation-based FDR). Likewise for the mouse interactome, the candidate TBC1D4 interactors were required to be enriched (>1.5-fold change and significant on a 5% FDR level) in the WT samples compared with the TBC1D4-KO samples.

Excluding Unspecific Proteins

To exclude proteins unspecifically immunoprecipitated by the TBC1D4 antibody in the human muscle IP reactions, we compared the list of human TBC1D4 interactors to all the proteins identified in the mouse TBC1D4 interactome. Here, human TBC1D4 interactors were excluded as unspecific binders, if they were quantified in the mouse WT IP samples by <1.5-fold change to the TBC1D4-KO IP samples.

Statistical Analysis of Western Blot Analyses

Paired *t* test was performed on data shown in Figs. 3 and 4, and two-way repeated-measures ANOVA with Tukey and Šidák post hoc analysis were performed on data shown in Figs. 5 and 6, respectively.

Significant With Insulin Stimulation

Log_2 LFQ intensities of interactors were normalized to LFQ intensities of TBC1D4 in each sample. The Student *t* test was performed, and differences in means were considered significant when $P < 0.05$. In addition, an interactor was considered regulated by insulin if found exclusively in basal or insulin-stimulated samples (at least four of six samples). Due to a harsh cutoff point, proteins were allowed to be identified in one sample of the other condition (e.g., poly [ADP-ribose] polymerase [TIPARP] was identified in four insulin-stimulated samples and in one basal sample).

Data and Resource Availability

The MS proteomics data have been deposited to the ProteomeXchange Consortium via the Proteomics Identification Database (PRIDE) partner repository with the data set identifier PXD026225 (30).

RESULTS

Identification of Endogenous TBC1D4 Interacting Partners in Human Skeletal Muscle

To identify protein interactors of TBC1D4 in skeletal muscle, we performed a comprehensive proteomics workflow. This included IP of TBC1D4 from skeletal muscle obtained from healthy, young, lean individuals before and 2 h after a physiological hyperinsulinemic (~117 μIU/mL)-euglycemic clamp (Fig. 1*A*). In parallel, IP of TBC1D4 from muscle of TBC1D4-WT and whole-body TBC1D4-KO mice obtained in the basal state was performed (Fig. 1*B*). A principal component analysis revealed that the proteins identified in the TBC1D4 IP samples clustered together and were separated from those observed in the IgG control samples (Fig. 1*C*, left panel). Furthermore, the IP reactions in muscle from TBC1D4-WT and -KO mice clustered separately (Fig. 1*C*, right panel). As expected, TBC1D4 was highly enriched in the TBC1D4 antibody-specific IP of human samples as well as WT mouse samples (Fig. 1*D* and *E*). In the human TBC1D4 interactome, we identified 149 proteins as significant in the TBC1D4 IP compared with the IgG control based on the Student *t* test (FDR <5% and fold change >1.5) and/or by exclusive identification in at least 50% of the TBC1D4 IP samples. In the mouse TBC1D4 interactome, 109 proteins were identified as candidate interactors based on the Student *t* test (FDR <5% and fold change >1.5 in WT vs. TBC1D4 KO) and/or by exclusive identification in at least 50% of WT samples (Supplementary Table 1). To exclude proteins captured by unspecific antibody binding in the human TBC1D4 interactome, we used information from the TBC1D4 mouse interactome. If a significant human TBC1D4 interactor was found with <1.5-fold change of the mean difference between mouse WT and TBC1D4-KO samples, it was considered an unspecific binding partner. Of 149 significant human TBC1D4 interactors, 73 were ascribed to antibody cross-reactivity and 76 as being coimmunoprecipitated through TBC1D4 (Fig. 1*D* and Table 1). Of the 76 candidate human TBC1D4 interactors, 12 were found to have increased binding to TBC1D4 after insulin stimulation (exclusive identification or $P < 0.05$) (Fig. 1*F*). This included α-actinin-4 (ACTN4) and the various 14-3-3 protein isoforms previously implicated in the regulation of insulin-stimulated GLUT4 translocation (14,31).

Surprisingly, only four proteins were identified as statistically significant TBC1D4 interactors in both the human and mouse skeletal muscle (Fig. 1*G*). These included TBC1D1,

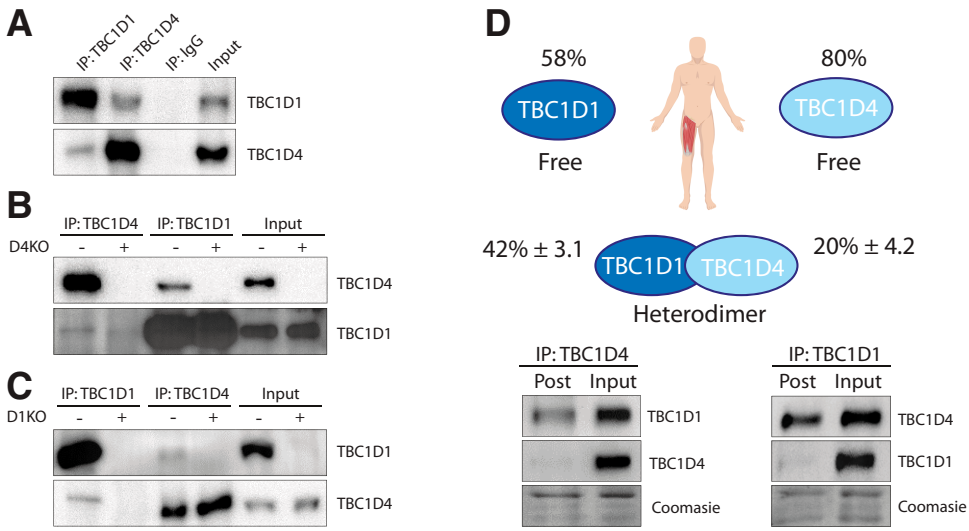

Figure 2—TBC1D1 and TBC1D4 interact in skeletal muscle tissue. Western blot analysis of TBC1D4 and TBC1D1 co-IP in human skeletal muscle (*A*), WT and TBC1D4 (D4KO) tibialis anterior muscle (*B*), and WT and TBC1D1 KO (D1KO) tibialis anterior muscle (*C*). *D*: Estimation of the TBC1D1 and TBC1D4 fraction bound to each other by comparing post-IP (supernatant after IP) to input (lysate before IP). Mean percentage is represented with SEM values (n = 19).

UGP2 (UTP–glucose-1-phosphate uridylyltransferase), YWHAG (14-3-3γ), and the protein VCP (transitional endoplasmic reticulum ATPase, also known as p97). Of those, only the 14-3-3γ–TBC1D4 protein interaction was regulated by insulin stimulation in human skeletal muscle, in line with previous observations in rat adipocytes (32). This interaction and its regulation with insulin stimulation serve as a proof-of-concept of our proteomics approach and is, to our knowledge, the first evidence of a 14-3-3 isoform-specific regulation under in vivo conditions.

Validation of the TBC1D1 and TBC1D4 Interaction in Skeletal Muscle Tissue

We identified TBC1D1 to be highly enriched in the human TBC1D4 IP (Fig. 1*D*). Additionally, TBC1D1 was identified in the TBC1D4 IP from WT mouse muscle but not from TBC1D4-KO muscle (Supplementary Table 1). It was recently shown that ectopically tagged TBC1D1 and TBC1D4 transfected into cultured cells are able to interact (33). In contrast, TBC1D4 was not found to coprecipitate with flag-TBC1D1 in a recent study in C2C12 cells (34). This is likely due to the low expression levels of TBC1D4 in C2C12 myotubes compared with mature mouse skeletal muscle (35). We confirmed by Western blotting that TBC1D1 and TBC1D4 coimmunoprecipitated in human skeletal muscle (Fig. 2*A*). The finding was not due to antibody cross-reactivity, as the anti-TBC1D4 antibody did not coimmunoprecipitate TBC1D1 from muscle of the TBC1D4-KO mouse (Fig. 2*B*). Similarly, the anti-TBC1D1 antibody did not coimmunoprecipitate TBC1D4 from muscle of the TBC1D1-KO mouse (Fig. 2*C*). We did not detect alterations in the abundance of TBC1D4 and TBC1D1 protein in muscle from TBC1D1- and TBC1D4-KO mice, respectively (Fig. 2*B* and *C*). By comparing the supernatant fraction of the TBC1D1 and TBC1D4 IP (post) to the muscle lysate before IP (input), we estimated that ∼42% of all TBC1D1 co-IP with TBC1D4 and ∼20% of all TBC1D4 co-IP with TBC1D1 in human skeletal muscle (Fig. 2*D*). As we show that relatively large proportions of the two RabGAPs interact in human skeletal muscle, we sought to investigate the phosphoregulation of the TBC1D1-TBC1D4 complex in human skeletal muscle in response to insulin and exercise.

Intact Insulin- and Exercise-Mediated Phosphorylation of TBC1D1 in Complex With TBC1D4 in Human Skeletal Muscle

MS analyses did not indicate any changes of the protein levels in the TBC1D1-TBC1D4 interaction following hyperinsulinemic (∼117 μIU/mL)-euglycemic clamp conditions in skeletal muscle of young healthy individuals (Table in Fig. 1*G*). This was further examined by co-IP and immunoblot analyses in a larger (n = 11) independent cohort studied under similar clamp conditions (insulin ∼115 μIU/mL). In this cohort, insulin induced a robust increase in pAkt at Ser473 and Thr308, signifying activation of the canonical insulin signaling pathway (Supplementary Fig. 1*A* and *B*). The TBC1D4-TBC1D1 protein interaction was not significantly different when comparing the complex before and after the insulin stimulation (Fig. 3*A*). The major insulin- and Akt-regulated phosphorylation site on TBC1D1, Thr596, was assessed in the TBC1D1-TBC1D4 complex in response to insulin stimulation. For the input samples, we found a significant increase in the phosphorylation of Thr596 (Fig. 3*B*). In the TBC1D1-TBC1D4 complex, phosphorylation of Thr596 also increased in 9 of the 11 subjects. Even though this did not reach statistical significance

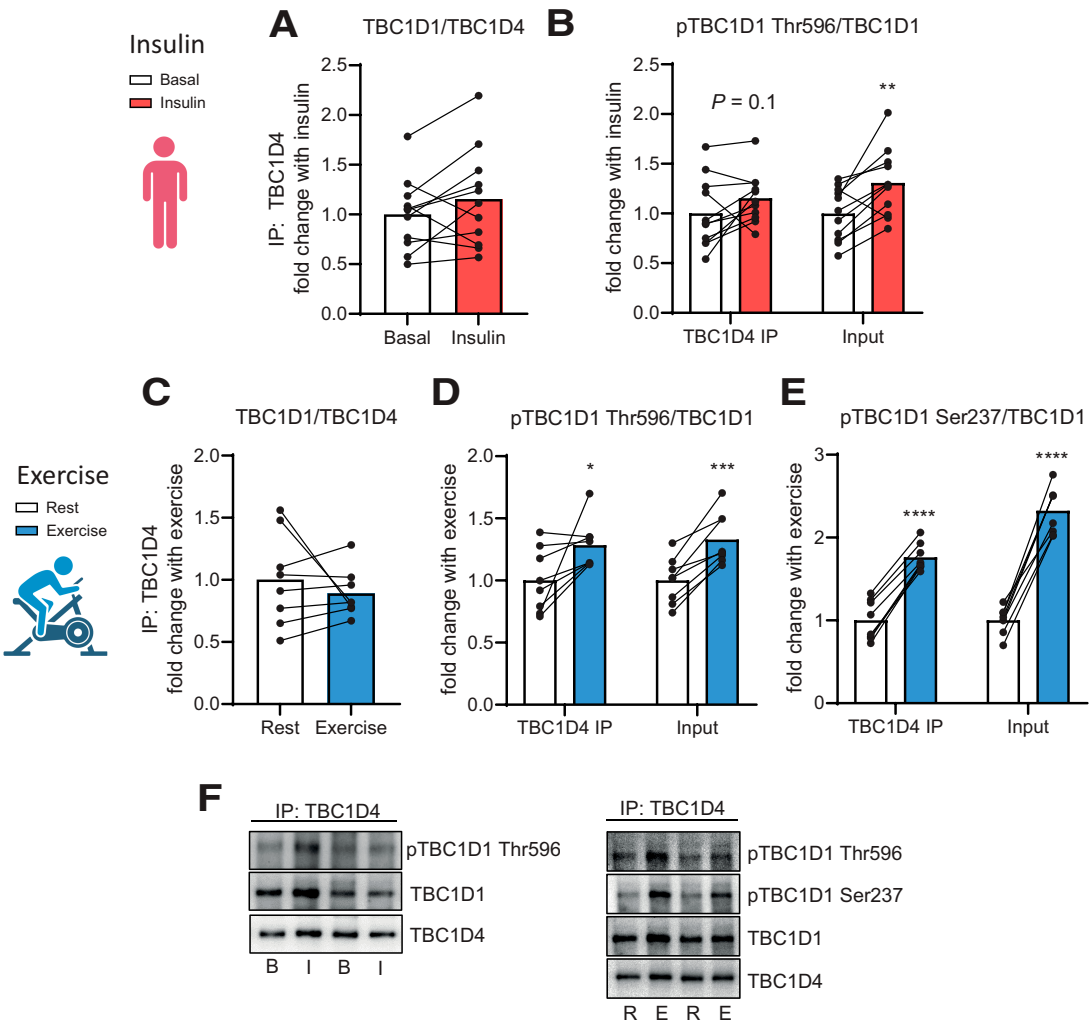

Figure 3—Intact insulin- and exercise-mediated phosphorylation of TBC1D1 in complex with TBC1D4. IP of TBC1D4 from basal and insulin-stimulated human skeletal muscle, followed by Western blot of TBC1D1 total (*A*) and p-TBC1D1 Thr596 (*B*). IP of TBC1D4 from rested and acutely exercised human skeletal muscle, followed by Western blot of TBC1D1 total (*C*), pTBC1D1 Thr596 (*D*), and pTBC1D1 Ser237 (*E*). *F*: Representative Western blot of IP data. Input refers to muscle lysate before IP. Dots and lines represent individual responses ($n = 11$ in *A* and *B* and $n = 8$ in *C–E*). Data were analyzed by paired Student *t* test. ****$P < 0.0001$, ***$P < 0.001$, **$P < 0.01$, and *$P < 0.05$.

($P = 0.10$), we interpret the data to indicate that phosphorylation of Thr596 in response to insulin occurs independently of whether TBC1D1 is in complex with TBC1D4 or not.

In skeletal muscle, TBC1D1 undergoes phosphorylation in response to exercise. We previously showed that Ser237 and Thr596 on TBC1D1 are phosphorylated by AMPKα2-containing complexes in mouse muscle in response to exercise-like stimuli (i.e., contraction and AICAR) (27,36). To assess the regulation and phosphorylation pattern of TBC1D1 in complex with TBC1D4 during exercise, we immunoprecipitated TBC1D4 from muscle biopsy specimens obtained before and immediately after a single bout of high-intensity interval exercise from eight young healthy male subjects. Phosphorylation of AMPKα Thr172 was elevated threefold after the exercise session ($P < 0.001$), confirming exercise-induced signaling (Supplementary Fig. 1*C*). We found that the TBC1D1-TBC1D4 interaction was not regulated by acute exercise (Fig. 3*C*). Furthermore, phosphorylation of Thr596 and Ser237 on TBC1D1 in complex with TBC1D4 increased similarly compared with findings from the input samples (Fig. 3*D–F*). These data indicate that phosphorylation of TBC1D1 is induced by exercise independently of its interaction with TBC1D4.

Intact Insulin- and Exercise-Mediated Phosphorylation of TBC1D4 in Complex With TBC1D1 in Human Skeletal Muscle

In order to assess the phosphorylation signature of TBC1D4 bound to TBC1D1, we immunoprecipitated TBC1D1 from human skeletal muscle of young healthy male subjects before and after hyperinsulinemic (~115 mIU/mL)-euglycemic

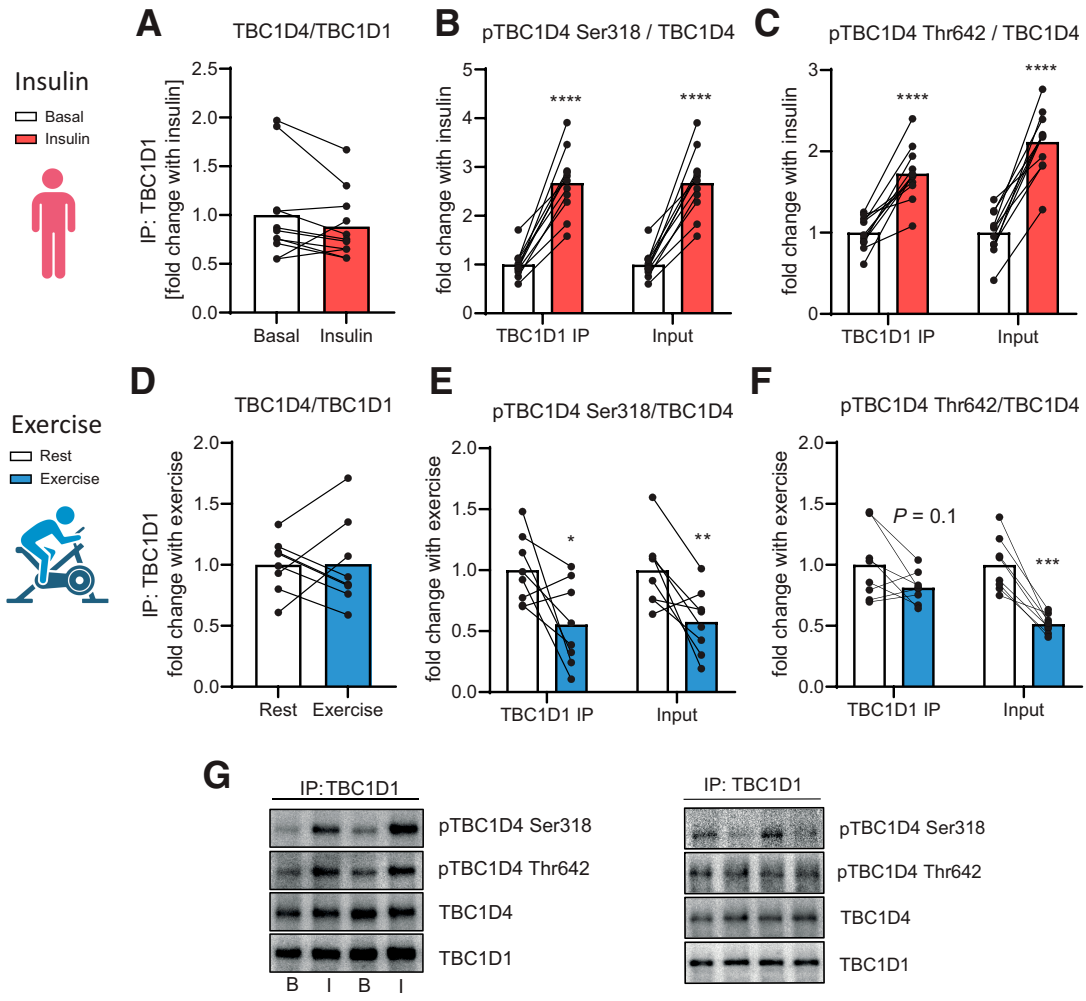

Figure 4—Intact insulin- and exercise-mediated phosphorylation of TBC1D4 in complex with TBC1D1. IP of TBC1D1 from basal (*B*) and insulin (I)-stimulated human skeletal muscle, followed by Western blot of TBC1D4 total (*A*), pTBC1D4 Ser318 (*B*), and pTBC1D4 Thr642 (*C*). IP of TBC1D1 from rested (R) and acutely exercised (*E*) human skeletal muscle, followed by Western blot of TBC1D4 total (*D*), pTBC1D4 Ser318 (*E*), and pTBC1D4 Thr642 (*F*). *G*: Representative Western blot of IP data. Input refers to muscle lysate prior to IP. Dots and lines represent individual responses ($n = 11$ in *A–C* and $n = 8$ D-F). Data were analyzed by paired Student *t* test. $^{****}P < 0.0001$, $^{***}P < 0.001$, $^{**}P < 0.01$, and $^{*}P < 0.05$.

clamp. This did not reveal any net alteration in the TBC1D4-TBC1D1 interaction upon insulin stimulation (Fig. 4*A*), confirming our previous findings from the TBC1D4 IP (Fig. 3*A*). We then investigated two major Akt phosphorylation sites on TBC1D4, Ser318 and Thr642, which are proposed to be critical for GLUT4 translocation (37). We found that phosphorylation of TBC1D4 at Ser318 and Thr642 increased to a similar extent in response to insulin stimulation independently of its interaction with TBC1D1 (Fig. 4*B* and *C*).

To test whether the exercise-induced phosphorylation of TBC1D4 was affected by the binding to TBC1D1, we immunoprecipitated TBC1D1 from protein lysates of rested and acutely exercised skeletal muscle of young healthy male subjects. We confirmed that an acute bout of high-intensity exercise did not alter the net TBC1D4-TBC1D1 interaction (Fig. 4*D*). Phosphorylation of TBC1D4 Ser318 decreased with exercise. This occurred to a similar extent on the fraction bound to TBC1D1 and on that found in the input sample (Fig. 4*E*). Similarly, phosphorylation of Thr642 decreased with exercise in the input lysate, although this did not reach significance in the fraction bound to TBC1D1 (Fig. 4*F*). To establish whether phosphorylation of TBC1D4 Thr642 is indeed decreased upon exercise when in complex with TBC1D1, we repeated the TBC1D1 IP in lysates of muscles from the same subjects at rest and immediately after a session of moderate continuous exercise. We confirmed that phosphorylation of TBC1D4 at Ser318 and Thr642 decreased in response to exercise both in input samples and when bound to TBC1D1 (Supplementary Fig. 2*A–C*). A decrease in the phosphorylation of TBC1D4 at Ser318 and Thr642 following exercise is likely related to a drop in

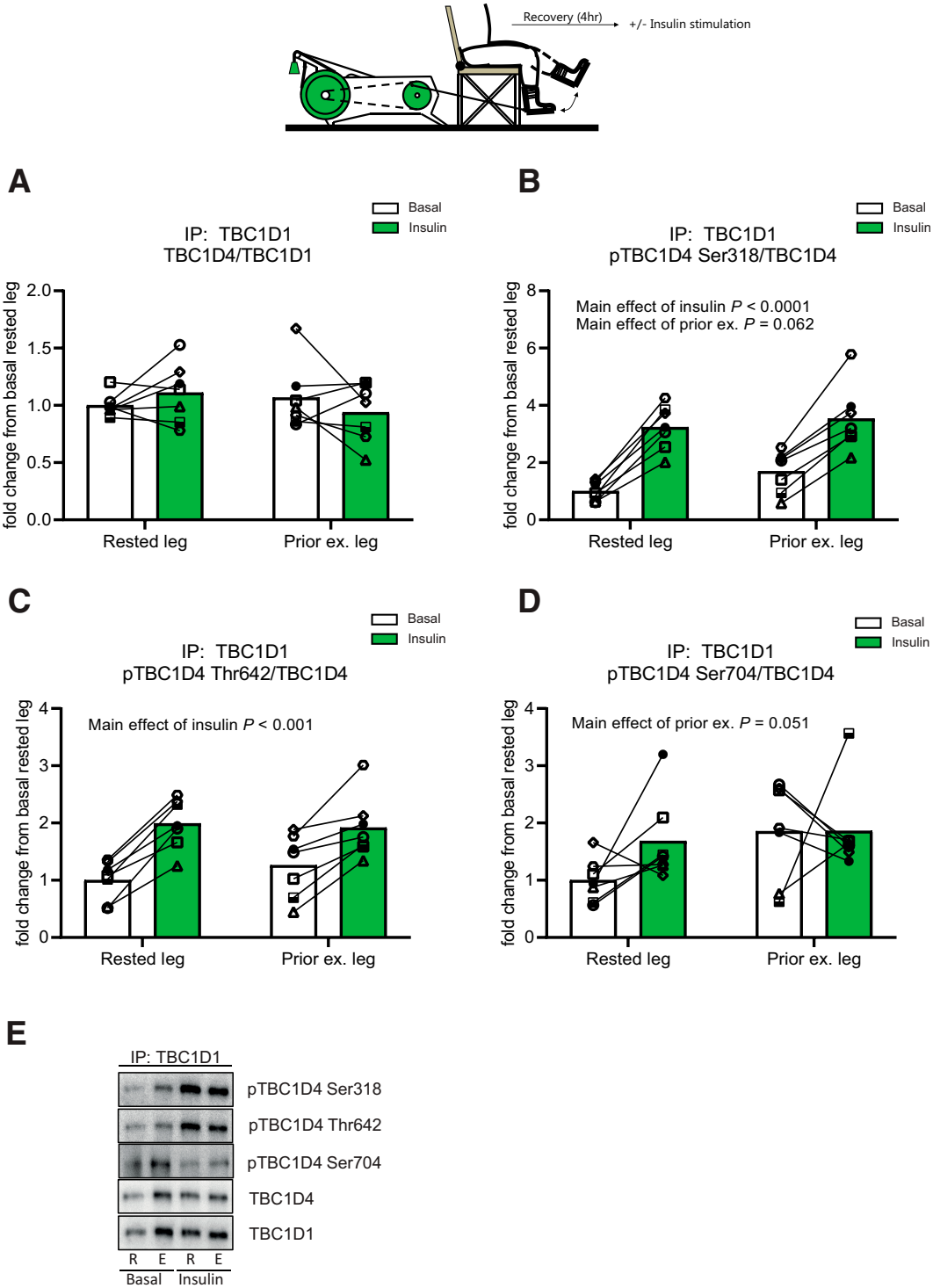

Figure 5—Insulin-stimulated phosphorylation of the TBC1D1-TBC1D4 complex after exercise. IP of TBC1D1 from rested (*R*) and prior exercised (*E*) human skeletal muscle at basal (*B*) and in response to insulin (*I*) stimulation, followed by Western blot of TBC1D4 total (*A*), pTBC1D4 Ser318 (*B*), pTBC1D4 Thr642 (*C*), and pTBC1D4 Ser704 (*D*). *E*: Representative Western blot of IP data. Data were analyzed by repeated-measures ANOVA. ANOVA significance is displayed with text on each graph. Values for each individual are marked with a unique asterisk and connected with lines within each leg ($n = 7$).

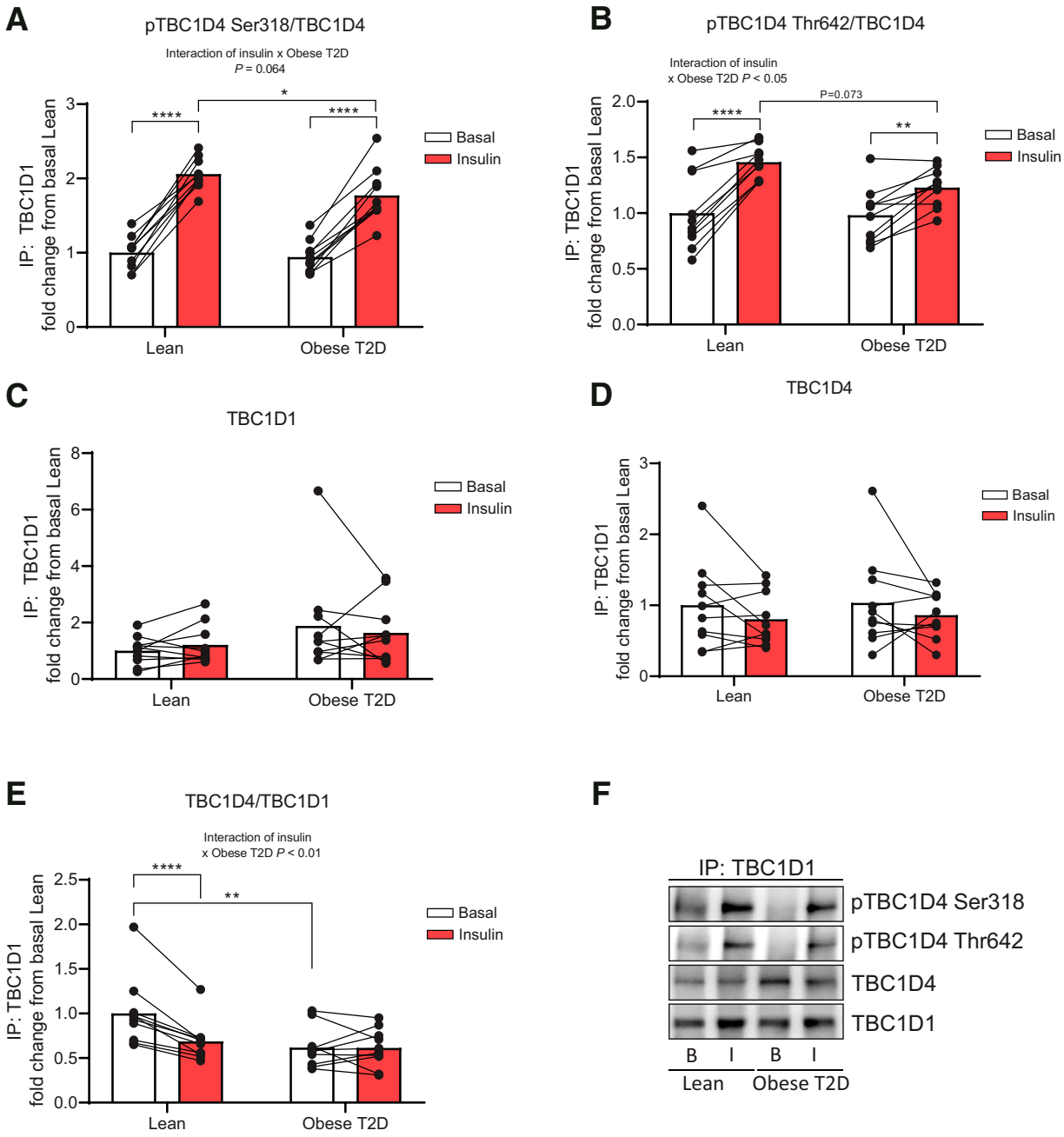

Figure 6—Insulin-stimulated regulation of the TBC1D1-TBC1D4 complex in skeletal muscle from healthy, lean individuals and obese individuals with type 2 diabetes. IP of TBC1D1 from basal and insulin-stimulated human skeletal muscle in healthy, lean individuals and obese individuals with type 2 diabetes, followed by Western blot of p-TBC1D4 Ser318 (*A*), p-TBC1D4 Thr642 (*B*), TBC1D1 total (*C*) and TBC1D4 (*D*). *E*: Ratio of TBC1D4 co-IP to TBC1D1 IP. Representative Western blot of IP data. Bars are means and lines represent individual responses (n = 10). Data were analyzed by two-way repeated-measures ANOVA within group. ANOVA significance is displayed with text on each graph. Šidák multiple comparisons test was used as post hoc test. ****$P < 0.0001$, **$P < 0.01$, and *$P < 0.05$.

plasma insulin levels that typically follows whole-body exercise (38).

Preserved Insulin-Stimulated Phosphorylation of the TBC1D1-TBC1D4 Complex in the Period Following Exercise in Human Skeletal Muscle

A single bout of exercise has been shown to enhance insulin-stimulated glucose uptake in skeletal muscle (39–41). We and others have shown in rodents that this correlates well with the phosphorylation of TBC1D4 (42,43), and we recently showed in transgenic mice that TBC1D4 is required for this process (12). To clarify whether the insulin-stimulated phosphorylation of TBC1D4 bound to TBC1D1 was affected in the period following exercise, we took advantage of the one-legged knee extensor exercise model in a young healthy cohort. Four hours following a single bout of

Table 1—List of 76 significant TBC1D4 interactors in human skeletal muscle

Gene name	Significance based on	Gene name	Significance based on
ABCE1	Exclusive	MYL6B	*t* test
ACTL6A	Exclusive + *t* test	MYLPF	*t* test
ACTN4	Exclusive	NDUFA1	Exclusive
ALDH3A2	Exclusive	PFDN4	*t* test
APOBEC2	Exclusive	PHTF2	Exclusive
ARF1	Exclusive	PNKD	Exclusive
ARID1A	*t* test	PRRC2A	Exclusive + *t* test
ATAD3A	*t* test	PSMC6	Exclusive
ATP2A2	*t* test	RANBP2	Exclusive
BCAP29	Exclusive + *t* test	RPN1	Exclusive
C17orf85	Exclusive + *t* test	RTN2	Exclusive
CAPN1	Exclusive	SAMHD1	Exclusive + *t* test
CIRBP	Exclusive	SEC23IP	Exclusive + *t* test
COL6A1	Exclusive	SECTM1	Exclusive
DDB1	Exclusive	SFXN1	Exclusive
DHRS7	Exclusive	SFXN4	Exclusive
FECH	Exclusive	SGCD	Exclusive
GPBP1	Exclusive	SLC2A1	Exclusive
HIST1H2AC	Exclusive	SMARCA2	*t* test
HRG	Exclusive	SMARCB1	Exclusive
HSDL2	Exclusive	SMARCC2	*t* test
HSPA6	Exclusive + *t* test	SMARCD3	*t* test
HSPE1-MOB4	Exclusive + *t* test	SNX9	Exclusive + *t* test
IGFN1	*t* test	STRIP2	Exclusive + *t* test
IGHV4-61	Exclusive	TAX1BP1	Exclusive + *t* test
LARP1	Exclusive + *t* test	TBC1D1	Exclusive + *t* test
LEMD2	Exclusive	TIPARP	Exclusive + *t* test
MAPT	Exclusive + *t* test	TXLNB	Exclusive
MORC2	Exclusive + *t* test	UGP2	Exclusive
MTX2	Exclusive	UNC45B	Exclusive + *t* test
MUSTN1	Exclusive	USP5	Exclusive
MYH13	Exclusive + *t* test	VCP	Exclusive
MYH2	*t* test	WDR44	Exclusive
MYH3	*t* test	YTHDF3	Exclusive
MYH4	*t* test	YWHAE	Exclusive + *t* test
MYH7	*t* test	YWHAG	*t* test
MYL1	*t* test	ZCCHC11	Exclusive + *t* test
MYL2	*t* test	ZNF638	Exclusive + *t* test

Significance was based on exclusive identification and/or on Student *t* test (>1.5-fold change D4IP vs. IgG and FDR <0.05). See RESEARCH DESIGN AND METHODS for details.

endurance-like one-legged exercise, biopsy specimens were obtained from vastus lateralis of both legs. Then the subjects underwent a hyperinsulinemic (~117 μIU/mL)-euglycemic clamp for 2 h, and a new set of muscle specimens was obtained. The TBC1D1-TBC1D4 protein interaction was not affected 4 h into exercise recovery or by the following 2-h insulin stimulation (Fig. 5*A*). Phosphorylation of TBC1D4 at Ser318 and Thr642 increased with insulin,

whereas Ser704 increased in the prior exercised muscle in both of the TBC1D1 IPs (Fig. 5*B–E*) and in the input samples (Supplementary Fig. 3*A–D*). However, we did not detect differences in the phosphorylation status of TBC1D4 in the co-IP samples compared with the input samples.

Dysregulated TBC1D1-TBC1D4 Interaction in Skeletal Muscle From Middle-Aged Obese Individuals With Type 2 Diabetes

Impaired muscle insulin signaling at the level of Akt and TBC1D4 has been shown to diminish glucose uptake in skeletal muscle (4,26,44–46). To illuminate whether the interaction between TBC1D1 and TBC1D4 was altered by type 2 diabetes, we investigated a cohort of obese middle-aged (50 ± 1 years) individuals with type 2 diabetes and compared the effect of insulin to that observed in a lean, healthy, age-matched control group. Following a 4-h hyperinsulinemic (∼54 μU/mL)-euglycemic clamp, insulin-stimulated phosphorylation of Akt at Ser473 (∼40%) and Thr308 (∼55%) was reduced in input muscle lysates from the obese individuals with type 2 diabetes compared with the control group (Supplementary Fig. 4*A* and *B*). Similarly, insulin-stimulated phosphorylation of TBC1D4 at Ser318 (P = 0.001) and Thr642 (P = 0.061) was decreased (Supplementary Fig. 4*C* and *D*), thereby demonstrating suppressed Akt-TBC1D4 signaling in obese individuals with type 2 diabetes. Interestingly, the compromised insulin-stimulated phosphorylation of TBC1D4 Thr642 was also present on the part of TBC1D4 bound to TBC1D1 that also appeared to be valid for Ser318 (P = 0.064) (Fig. 6*A* and *B*). Although the IP of TBC1D1 and co-IP of TBC1D4 were not significantly changed with insulin stimulation or different between groups (Fig. 6*C* and *D*), the ratio of bound TBC1D4 to TBC1D1 was differentially regulated between groups upon insulin stimulation (Fig. 6*E*). Thus, TBC1D4 dissociated from TBC1D1 in response to insulin in the lean group, whereas no change was observed in the obese group with type 2 diabetes. Furthermore, the TBC1D4-to-TBC1D1 ratio in the basal state was decreased in the obese group with type 2 diabetes compared with the lean control group.

DISCUSSION

The current study investigated the endogenous TBC1D4 interactome in mature skeletal muscle. We identified 76 candidate human TBC1D4 interactors whereof the binding of 12 was regulated by insulin stimulation. One of them included ACTN4, which interacted with TBC1D4 in response to insulin. Interestingly, ACTN4 is known to directly interact with GLUT4 in an insulin-dependent manner (31,47). Knockdown of ACTN4 in L6 myotubes prevents the insulin-elicited anchoring of GLUT4 to actin cytoskeleton that decreases plasma membrane GLUT4 content (31). Our observations, which indicate that ACTN4 and TBC1D4 interact upon insulin stimulation, suggest a role for TBC1D4 in anchoring GLUT4 vesicles to the near-membrane actin cytoskeleton. We also identified several novel interactors, such as the ADP-ribosylation factor 1 (ARF1), a GTP-binding protein involved in vesicle trafficking, and SECTM1, a small, secreted protein with implication in tumor-immune cell communication. The biological effects of these interactions are unknown. Intriguingly, we did not detect some of the formerly and characterized substrates of TBC1D4, including IRAP and various Rab proteins (48,49). This may be related to the washing protocol used during the IP procedure, which could disrupt weak and transient protein interactions. In addition, a stringent P value correction might also mask true interactors, as indicated for Rab10 that was identified but did not reach statistical significance in the mouse TBC1D4 interactome (FDR = 0.13).

UGP2 (UDP-glucose pyrophosphorylase), an essential enzyme in the glycogen synthesis pathway, was found to interact with TBC1D4 in both mouse and human skeletal muscle. Given our recent work showing that AMPK regulates UGP2 expression in skeletal muscle (50) and that AMPK has been coupled to the regulation of glucose uptake, glycogen storage, and phosphorylation of TBC1D4 (7,22,43), we propose a trilateral relationship between AMPK, UGP2, and TBC1D4 that may be involved in partitioning the glucose taken up toward glycogen synthesis (50). We also identified VCP in both human and mouse muscle to interact with TBC1D4. VCP has been reported to regulate vesicle trafficking, including sorting of ubiquitinated cargo into endolysosomes for degradation (51). The latter is of particular interest, as TBC1D4 has been shown to regulate GLUT4 protein degradation in skeletal muscle through the lysosomal pathway (52).

We identified TBC1D1 as a bona fide TBC1D4 interaction partner in human and mouse skeletal muscle. Although prior findings have shown that TBC1D4 homodimerization does not affect TBC1D4 RabGAP catalytic activity in vitro, it is possible that heterodimerization of TBC1D4 and TBC1D1 is associated with a change in the activity of the two independent RabGAPs (53). Clearly, this needs further clarification, but intact phosphorylation of the TBC1D4-TBC1D1 complex may argue against such suggestion.

TBC1D4 has been linked to endosomal sorting of GLUT4 into an insulin-sensitive secretory compartment (54,55). It can be speculated that the TBC1D1-TBC1D4 complex regulates the GLUT4 sorting into the insulin-sensitive secretory compartment and that the TBC1D4-TBC1D1 complex stoichiometry controls the size and/or flux of this GLUT4 protein pool. When we investigated this interaction in obese patients with type 2 diabetes and in lean, healthy, age-matched control subjects, we found that the TBC1D4-TBC1D1 complex dissociated in the middle-aged control group in response to insulin, whereas this response was absent in the group with diabetes, which, however, exhibited overall reduced levels of the TBC1D4-TBC1D1 complex. The insulin-induced TBC1D4-TBC1D1 complex dissociation in the age-matched control group stands in contrast to our

findings in healthy, young, lean subjects (Figs. 3–5). This discrepancy may be explained by differences in the two study designs, including length of the insulin stimulation that may be critical for the dissociation to take place. Assuming that the TBC1D4-TBC1D1 complex maintains GLUT4 sorting into an insulin-sensitive secretory compartment, our data would suggest that young healthy individuals have a higher sorting capacity compared with healthy older individuals. Moreover, the reduced levels of TBC1D4-TBC1D1 complexes in individuals with type 2 diabetes may indicate chronic depletion of GLUT4 in the insulin-sensitive secretory compartment. Together, this may contribute to muscle insulin resistance that is a hallmark in both aging and type 2 diabetes (1). Whether this holds true is currently unknown and thus needs further investigations under proper matched conditions.

Recent work has shown that AMPK- and Akt-mediated phosphorylation of TBC1D4 regulates binding with 14-3-3γ protein and IRAP but does not regulate the GAP activity of TBC1D4 in vitro (56). Similar results have been reported for TBC1D1 (57). This suggests that phosphorylation and/or protein interactions of TBC1D1 and TBC1D4 promote a change in their localization away from compartments rich in certain GTP-bound substrates (e.g., Rab proteins), leading to enhanced GLUT4 translocation. Based on this, it may be speculated that insulin-regulated protein interactions of TBC1D4, including those described in the current study, could contribute to TBC1D4 localization and hence regulation of glucose uptake in skeletal muscle.

In conclusion, we provide new insight into TBC1D4 signaling by mapping its protein interactors in human and mouse skeletal muscle. We find several novel interactors to which their protein association with TBC1D4 increased during in vivo insulin stimulation. Additionally, we reveal that TBC1D1 is an endogenous binding partner of TBC1D4 in human skeletal muscle, suggesting direct cooperative action through a heterodimer complex. Interestingly, the TBC1D1-TBC1D4 interaction seems to be compromised in type 2 diabetes and may be affected by age. Since aging and type 2 diabetes are associated with muscle insulin resistance, we propose that the stoichiometry of free and complex-bound TBC1D1 and TBC1D4 is a determining factor for the regulation of muscle glucose uptake and insulin sensitivity in humans.

Acknowledgments. The authors would like to thank Dr. Laurie J. Goodyear (Joslin Diabetes Center and Harvard Medical School, Boston, MA) for the donation of phosphospecific TBC1D4-Ser711 antibody. The authors acknowledge the mass spectrometry platform staff (University of Copenhagen, Novo Nordisk Foundation Center for Protein Research, Clinical Proteomics) for their support with the proteomics analysis. The authors also thank Professor Erik A. Richter and Professor Bente Kiens (Department of Nutrition, Exercise and Sports, University of Copenhagen, Copenhagen, Denmark) for their expertise and assistance during several of the clinical experiments.

Funding. This work was supported by grants from the Danish Council for Independent Research (FSS: 610-00498B) and the Novo Nordisk Foundation (NNF210C0070370) given to J.F.P.W. This work was also supported by a postdoctoral research fellow grant to R.K. from the Danish Diabetes Academy, which is funded by the Novo Nordisk Foundation (grant number NNF17SA0031406). The proteomics analysis and A.S.D. were supported by the Novo Nordisk Foundation (NNF14CC001 and NNF18CC0034900).

Duality of Interest. J.F.P.W. has ongoing collaborations with Pfizer Inc. and Novo Nordisk Inc., unrelated to the current study. No other potential conflicts of interest relevant to this article were reported.

Author Contributions. J.K.L., J.F.P.W., and R.K. conceived and designed the study. J.K.L., M.R.L., and J.B.B. conducted laboratory analyses. J.K.L. and A.S.D. analyzed mass spectrometry data. J.F.P.W., J.K.L., D.E.S., J.R.H., K.H., and J.F.P.W. conducted clinical experiments. A.C. and H.A.-H. contributed animal resources. J.K.L., J.F.P.W., and R.K. drafted the manuscript. All authors wrote, reviewed, edited, and approved the manuscript. J.F.P.W. is the guarantor of this work and, as such, had full access to all the data in the study and takes responsibility for the integrity of the data and the accuracy of the data analysis.

References

1. Beck-Nielsen H. The role of glycogen synthase in the development of hyperglycemia in type 2 diabetes – 'To store or not to store glucose, that's the question'. Diabetes Metab Res Rev 2012;28:635–644

2. Huang C, Thirone ACP, Huang X, Klip A. Differential contribution of insulin receptor substrates 1 versus 2 to insulin signaling and glucose uptake in l6 myotubes. J Biol Chem 2005;280:19426–19435

3. Kane S, Sano H, Liu SCH, et al. A method to identify serine kinase substrates: Akt phosphorylates a novel adipocyte protein with a Rab GTPase-activating protein (GAP) domain. J Biol Chem 2002;277:22115–22118

4. Chen S, Wasserman DH, MacKintosh C, Sakamoto K. Mice with AS160/TBC1D4-Thr649Ala knockin mutation are glucose intolerant with reduced insulin sensitivity and altered GLUT4 trafficking. Cell Metab 2011;13:68–79

5. Manousaki D, Kent JW Jr, Haack K, et al. Toward precision medicine: TBC1D4 disruption is common among the Inuit and leads to underdiagnosis of type 2 diabetes. Diabetes Care 2016;39:1889–1895

6. Moltke I, Grarup N, Jørgensen ME, et al. A common Greenlandic TBC1D4 variant confers muscle insulin resistance and type 2 diabetes. Nature 2014;512:190–193

7. Kjøbsted R, Roll JLW, Jørgensen NO, et al. AMPK and TBC1D1 regulate muscle glucose uptake after, but not during, exercise and contraction. Diabetes 2019;68:1427–1440

8. An D, Toyoda T, Taylor EB, et al. TBC1D1 regulates insulin- and contraction-induced glucose transport in mouse skeletal muscle. Diabetes 2010; 59:1358–1365

9. Stone S, Abkevich V, Russell DL, et al. TBC1D1 is a candidate for a severe obesity gene and evidence for a gene/gene interaction in obesity predisposition. Hum Mol Genet 2006;15:2709–2720

10. Meyre D, Farge M, Lecoeur C, et al. R125W coding variant in TBC1D1 confers risk for familial obesity and contributes to linkage on chromosome 4p14 in the French population. Hum Mol Genet 2008;17:1798–1802

11. Treebak JT, Frøsig C, Pehmøller C, et al. Potential role of TBC1D4 in enhanced post-exercise insulin action in human skeletal muscle. Diabetologia 2009;52:891–900

12. Kjøbsted R, Chadt A, Jørgensen NO, et al. TBC1D4 is necessary for enhancing muscle insulin sensitivity in response to AICAR and contraction. Diabetes 2019;68:1756–1766

13. Geraghty KM, Chen S, Harthill JE, et al. Regulation of multisite phosphorylation and 14-3-3 binding of AS160 in response to IGF-1, EGF, PMA and AICAR. Biochem J 2007;407:231–241

14. Ramm G, Larance M, Guilhaus M, James DE. A role for 14-3-3 in insulin-stimulated GLUT4 translocation through its interaction with the RabGAP AS160. J Biol Chem 2006;281:29174–29180

15. Mîinea CP, Sano H, Kane S, et al. AS160, the Akt substrate regulating GLUT4 translocation, has a functional Rab GTPase-activating protein domain. Biochem J 2005;391:87–93
16. Hein MY, Hubner NC, Poser I, et al. A human interactome in three quantitative dimensions organized by stoichiometries and abundances. Cell 2015;163:712–723
17. Thomas EC, Hook SC, Gray A, et al. Isoform-specific AMPK association with TBC1D1 is reduced by a mutation associated with severe obesity. Biochem J 2018;475:2969–2983
18. Cox J, Mann M. MaxQuant enables high peptide identification rates, individualized p.p.b.-range mass accuracies and proteome-wide protein quantification. Nat Biotechnol 2008;26:1367–1372
19. Tyanova S, Temu T, Sinitcyn P, et al. The Perseus computational platform for comprehensive analysis of (prote)omics data. Nat Methods 2016;13:731–740
20. Steenberg DE, Jørgensen NB, Birk JB, et al. Exercise training reduces the insulin-sensitizing effect of a single bout of exercise in human skeletal muscle. J Physiol 2019;597:89–103
21. Steenberg DE, Hingst JR, Birk JB, et al. A single bout of one-legged exercise to local exhaustion decreases insulin action in nonexercised muscle leading to decreased whole-body insulin action. Diabetes 2020;69:578–590
22. Hingst JR, Bruhn L, Hansen MB, et al. Exercise-induced molecular mechanisms promoting glycogen supercompensation in human skeletal muscle. Mol Metab 2018;16:24–34
23. Kristensen DE, Albers PH, Prats C, Baba O, Birk JB, Wojtaszewski JFP. Human muscle fibre type-specific regulation of AMPK and downstream targets by exercise. J Physiol 2015;593:2053–2069
24. Højlund K, Birk JB, Klein DK, et al. Dysregulation of glycogen synthase COOH- and NH2-terminal phosphorylation by insulin in obesity and type 2 diabetes mellitus. J Clin Endocrinol Metab 2009;94:4547–4556
25. Bergström J. Muscle electrolytes in man determined by neutron activation analysis on needle biopsy specimens: a study on normal subjects, kidney patients, and patients with chronic diarrhoea. Scand J Clin Lab Invest 1962;14(Suppl. 68):11–13
26. Chadt A, Immisch A, de Wendt C, et al. Deletion of both Rab-GTPase–activating proteins TBC1D1 and TBC1D4 in mice eliminates insulin- and AICAR-stimulated glucose transport [published correction appears in Diabetes 2015;64:1492]. Diabetes 2015;64:746–759
27. Kjøbsted R, Treebak JT, Fentz J, et al. Prior AICAR stimulation increases insulin sensitivity in mouse skeletal muscle in an AMPK-dependent manner. Diabetes 2015;64:2042–2055
28. Treebak JT, Taylor EB, Witczak CA, et al. Identification of a novel phosphorylation site on TBC1D4 regulated by AMP-activated protein kinase in skeletal muscle. Am J Physiol Cell Physiol 2010;298:C377–C385
29. Turriziani B, Garcia-Munoz A, Pilkington R, Raso C, Kolch W, von Kriegsheim A. On-beads digestion in conjunction with data-dependent mass spectrometry: a shortcut to quantitative and dynamic interaction proteomics. Biology (Basel) 2014;3:320–332
30. Perez-Riverol Y, Csordas A, Bai J, et al. The PRIDE database and related tools and resources in 2019: improving support for quantification data. Nucleic Acids Res 2019;47:D442–D450
31. Talior-Volodarsky I, Randhawa VK, Zaid H, Klip A. α-Actinin-4 is selectively required for insulin-induced GLUT4 translocation. J Biol Chem 2008;283:25115–25123
32. Koumanov F, Richardson JD, Murrow BA, Holman GD. AS160 phosphotyrosine-binding domain constructs inhibit insulin-stimulated GLUT4 vesicle fusion with the plasma membrane. J Biol Chem 2011;286:16574–16582
33. Hatakeyama H, Morino T, Ishii T, Kanzaki M. Cooperative actions of Tbc1d1 and AS160/Tbc1d4 in GLUT4-trafficking activities. J Biol Chem 2019;294:1161–1172
34. Hook SC, Chadt A, Heesom KJ, et al. TBC1D1 interacting proteins, VPS13A and VPS13C, regulate GLUT4 homeostasis in C2C12 myotubes. Sci Rep 2020;10:17953
35. Deshmukh AS, Murgia M, Nagaraj N, Treebak JT, Cox J, Mann M. Deep proteomics of mouse skeletal muscle enables quantitation of protein isoforms, metabolic pathways, and transcription factors. Mol Cell Proteomics 2015;14:841–853
36. Treebak JT, Pehmøller C, Kristensen JM, et al. Acute exercise and physiological insulin induce distinct phosphorylation signatures on TBC1D1 and TBC1D4 proteins in human skeletal muscle. J Physiol 2014;592:351–375
37. Stöckli J, Davey JR, Hohnen-Behrens C, Xu A, James DE, Ramm G. Regulation of glucose transporter 4 translocation by the Rab guanosine triphosphatase-activating protein AS160/TBC1D4: role of phosphorylation and membrane association. Mol Endocrinol 2008;22:2703–2715
38. Wahren J, Felig P, Ahlborg G, Jorfeldt L. Glucose metabolism during leg exercise in man. J Clin Invest 1971;50:2715–2725
39. Wojtaszewski JFP, Hansen BF, Kiens B, Richter EA. Insulin signaling in human skeletal muscle: time course and effect of exercise. Diabetes 1997;46:1775–1781
40. Wojtaszewski JFP, Hansen BF, Gade J, et al. Insulin signaling and insulin sensitivity after exercise in human skeletal muscle. Diabetes 2000;49:325–331
41. Richter EA, Mikines KJ, Galbo H, Kiens B. Effect of exercise on insulin action in human skeletal muscle. J Appl Physiol (1985) 1989;66:876–885
42. Wang H, Arias EB, Pataky MW, Goodyear LJ, Cartee GD. Postexercise improvement in glucose uptake occurs concomitant with greater γ3-AMPK activation and AS160 phosphorylation in rat skeletal muscle. Am J Physiol Endocrinol Metab 2018;315:E859–E871
43. Kjøbsted R, Munk-Hansen N, Birk JB, et al. Enhanced muscle insulin sensitivity after contraction/exercise is mediated by AMPK. Diabetes 2017;66:598–612
44. Jaiswal N, Gavin MG, Quinn WJ III, et al. The role of skeletal muscle Akt in the regulation of muscle mass and glucose homeostasis. Mol Metab 2019;28:1–13
45. Arias EB, Zheng X, Agrawal S, Cartee GD. Whole body glucoregulation and tissue-specific glucose uptake in a novel Akt substrate of 160 kDa knockout rat model. PLoS One 2019;14:e0216236
46. Cho H, Mu J, Kim JK, et al. Insulin resistance and a diabetes mellitus-like syndrome in mice lacking the protein kinase Akt2 (PKBβ). Science 2001;292:1728–1731
47. Foster LJ, Rudich A, Talior I, et al. Insulin-dependent interactions of proteins with GLUT4 revealed through stable isotope labeling by amino acids in cell culture (SILAC). J Proteome Res 2006;5:64–75
48. Peck GR, Ye S, Pham V, et al. Interaction of the Akt substrate, AS160, with the glucose transporter 4 vesicle marker protein, insulin-regulated aminopeptidase. Mol Endocrinol 2006;20:2576–2583
49. Ishikura S, Bilan PJ, Klip A. Rabs 8A and 14 are targets of the insulin-regulated Rab-GAP AS160 regulating GLUT4 traffic in muscle cells. Biochem Biophys Res Commun 2007;353:1074–1079
50. Hingst JR, Kjøbsted R, Birk JB, et al. Inducible deletion of skeletal muscle AMPKα reveals that AMPK is required for nucleotide balance but dispensable for muscle glucose uptake and fat oxidation during exercise. Mol Metab 2020;40:101028
51. Ritz D, Vuk M, Kirchner P, et al. Endolysosomal sorting of ubiquitylated caveolin-1 is regulated by VCP and UBXD1 and impaired by VCP disease mutations. Nat Cell Biol 2011;13:1116–1123
52. Xie B, Chen Q, Chen L, Sheng Y, Wang HY, Chen S. The inactivation of RabGAP function of AS160 promotes lysosomal degradation of glut4 and causes postprandial hyperglycemia and hyperinsulinemia. Diabetes 2016;65:3327–3340
53. Woo JR, Kim S-J, Kim KY, Jang H, Shoelson SE, Park S. The carboxy-terminal region of the TBC1D4 (AS160) RabGAP mediates protein homodimerization. Int J Biol Macromol 2017;103:965–971

54. Brewer PD, Habtemichael EN, Romenskaia I, Coster ACF, Mastick CC. Rab14 limits the sorting of Glut4 from endosomes into insulin-sensitive regulated secretory compartments in adipocytes. Biochem J 2016;473:1315–1327

55. Brewer PD, Habtemichael EN, Romenskaia I, Mastick CC, Coster ACF. Insulin-regulated Glut4 translocation: membrane protein trafficking with six distinctive steps. J Biol Chem 2014;289:17280–17298

56. Eickelschulte S, Hartwig S, Leiser B, et al. AKT/AMPK-mediated phosphorylation of TBC1D4 disrupts the interaction with insulin-regulated aminopeptidase. J Biol Chem 2021;296:100637

57. Mafakheri S, Flörke RR, Kanngießer S, et al. AKT and AMP-activated protein kinase regulate TBC1D1 through phosphorylation and its interaction with the cytosolic tail of insulin-regulated aminopeptidase IRAP. J Biol Chem 2018;293:17853–17862